A Non-coherent UWB Direct Chaotic Ranging System for Precision Location and Positioning

*Wan-Cheol Yang, Sangyub Lee, Kwangdu Lee,
Kihwan Kim, Changsoo Yang and Haksun Kim

Wireless Solution Lab.
Samsung Electro-Mechanics Co. Ltd.(E-mail: wan-chul.yang @samsung.com)

Abstract

Precision location and positioning of Asset within a network is an attractive feature with various applications, especially in indoor environments. Such a demand is met by the standard task group, IEEE 802.15.4a. Several methods, that is, pulse, chirp and chaotic communications have been proposed so far to satisfy the requirements of the standard. Among them, ultra wideband direct chaotic communications has advantageous features such as low hardware complexity, low cost, lower power consumption and flexible frequency band plan. In this paper, the feasibility of the ranging system using non-coherent chaotic transceiver is investigated by designing and implementing the system and the performance is proved by conducting location experiments in real indoor environments.

Keywords: Ranging , Location , Positioning , OOK Receiver, UWB , Chaotic

1. Introduction

With the emergence of location-based applications, location finding techniques are becoming increasingly important [1]. Both indoor and outdoor coverage are required in the process of positioning. The Global Positioning System (GPS) delivers reliable radio frequency (RF) location using a combination of orbiting satellites to determine position coordinates. GPS works fine in most outdoor areas, but the satellite signals are not strong enough to penetrate inside most indoor environments. As a result, new indoor positioning technologies are beginning to appear on the market. Such technologies make use of 802.11 wireless LANs or Bluetooth, but the obtained accuracy is not good enough [2]. An alternative system that can provide the accuracy and robustness needed by indoor positioning systems and having an advantage of low power and low cost is the Ultra-Wideband (UWB) technology.

In general, positioning techniques exploit one or more characteristics of the radio signals to estimate the position of their sources. Some of the parameters that have been traditionally used for positioning are the received signal strength intensity (RSSI)[3], the angle of arrival (AOA)[4] and time of arrival (TOA). Among these positioning parameters, the RSSI is the least adequate for the UWB case, since it does not profit from the fine space-time resolution of impulsive signals and requires a site-specific path loss model [5]. The estimation of AOA, on the other hand, requires multiple antennas (or at least an antenna capable of beam forming) at the receiver. This requirement imply size and complexity needs that are often not compatible with the low-cost, small size constraints associated with the typical scenarios such as wireless sensor networks, envisioned for UWB technology. Given the reasons above, TOA stands out as the most suitable signal parameter to be used for positioning with UWB devices. Unfortunately, the estimation of the TOA of UWB signals in itself is not solved problem. For instance, correlation techniques, in conjunction with serial search, have been proposed for TOA estimation [6]. Special code design have also been considered as a means to facilitate the estimation of TOA with the correlation approach [7], and frequency-domain approaches have also been considered [8]. All the above solutions seem, nevertheless, to be in conflict with the strict requirements of low cost and low complexity imposed on some UWB applications such as wireless sensor networks. In order to reduce the complexity of UWB systems, non-coherent receivers such as energy collection have been recently proposed [9-10].

Recognizing these trends, the IEEE has established the IEEE 802.15.4a Task Group (TG), whose goal it is to develop a low complexity, low rate physical (PHY) layer standard with a precision ranging capability, and it has adopted UWB as the underlying technology. Low complexity, and thus low cost, of the devices is an important goal of the standard, and therefore it is required to enable UWB based ranging with non-coherent (energy detection) receivers. Though their performance (precision or reliability) will be less than that of coherent devices, the reduced cost justifies the tradeoff for many applications. Compare with IR(Impulse Radio) method[11-13], UWB direct chaotic communications has advantageous features such as low hardware complexity, low cost, lower power consumption, robustness in multi-path and flexible frequency band plan [14-17].

In this paper, the feasibility of the ranging application using non-coherent chaotic sources is investigated by designing and implementing the system. And the Two-Way Ranging (TWR) technique is applied to measure the signal round-trip time (RTT) between two asynchronous transceivers. To obtain high ranging accuracy in spite of using low clock rate and non-coherent receiving method, sophisticated designed counter-based ranging algorithm is proposed.

This paper is structured as follows. In section 2, a brief description of the system model is given. In section 3, the TWR-TOA based ranging algorithm is proposed. Real environments experimental results are given in section 4, followed by some concluding remarks in section 5.

2. Direct Chaotic Ranging System

The UWB radio communications can be viewed as an extreme form of spread spectrum communication systems. UWB radios transmit using very short impulses spread over a very large bandwidth. UWB radios are generally defined to have a fractional bandwidth η higher than 0.25 (i.e. a 3dB bandwidth which is at least 25% of the center frequency used).

$$\eta = \frac{2(f_H - f_L)}{(f_H + f_L)} \quad (1)$$

where f_H and f_L are high and low frequency respectively[17].

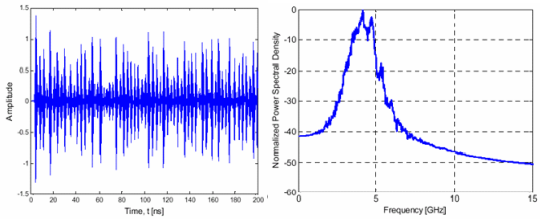

(a) (b)

Figure 1. Chaotic Signal. (a) time domain. (b) frequency domain.

Unlike IR UWB that uses short impulse signal, Chaotic signals are noise-like signals with ultra wideband frequency band as shown in Figure 1. Chaotic communications show highly advantageous features compared to general communications. First, hardware complexity is extremely low since chaotic signal can be generated directly into the desired microwave band through simple RF circuits. Thus, implementation cost is also very low, and power consuming extremely low and realizing efficient management of the battery. Second, in case of OOK(On Off Keying) modulation, BER performance against multipath is close to the AWGN. Last, pulse length is flexible while keeping the spectral bandwidth [14-17].

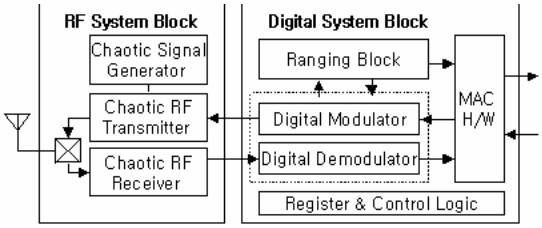

Figure 2. System Architecture.

The chaotic communication system consists of RF system block and digital system block as shown in Figure 2. And RF system block consists of Chaotic Signal Generator and Chaotic RF transceiver. Digital system block includes modulator, demodulator, control logic, ranging detection block and MAC hardware. Through ranging detection and MAC hardware with appropriate primitives, ranging data can be achieved and processed. Figure 3 shows the block diagram of Chaotic transceiver. The transmitter has modulator which generates the frame through MUX and multiplies the spreading code of 15 chips. And the chaotic RF signals, from the chaotic signal generator, are switched to produce On and Off modulation, the switch is directly controlled by from Modem system block. In the receiver, the OOK signals coming from the antenna are amplified into the detector diode. The detected envelope is sampled and fed into A/D. After the output of envelope detector goes through A/D, CDM code acquisition and tracking are followed for chip synchronization and dispreading. The reconstructed signal is stored in FIFO. Overall system architecture is enabling extremely small form factor as well as low power/low cost implementation.

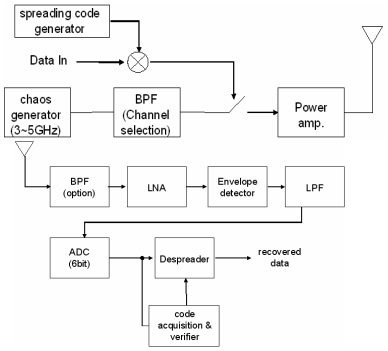

Figure 3. Chaotic Transceiver structure.

Chaotic signal has two distinguishing characteristics: 1) irregular phase variation and 2) wide bandwidth. When signals are overlapped in conventional communications, signals are distorted or cancelled out while in chaotic communications, signals can be kept as they are according to irregular phase characteristics. Moreover, the wide spectrum has the merit of power and spectral efficiency. Hence, when modulated as OOK, a simple transmitter with low power consumption can be built as shown in Figure 3 without the need of current-consuming PLL or frequency converter.

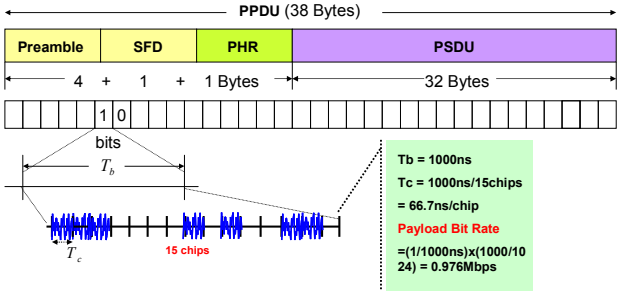

Figure 4. PHY Frame Structure.

Figure 4 shows the PHY frame structure consisting of preamble(4 bytes), SFD(1 byte), PHR(1 byte) and PSDU(32 bytes). T_b is pulse bit width or bit period as 1000 ns and T_c is chip period of 66.7 ns when maximum data rate of 1 Mbps is assumed. Therefore, payload bit rate can be calculated as

$$(1/1000ns)\times(1000/1024) = 0.976Mbps \quad (2)$$

3. Proposed Ranging Algorithm

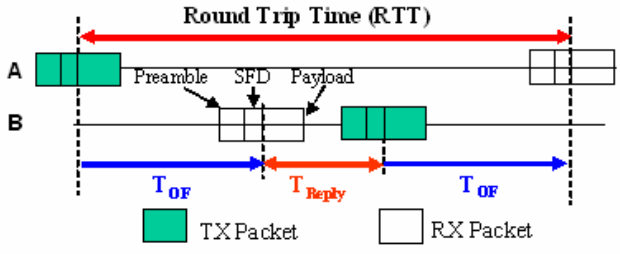

Figure 5. Two-way ranging procedure.

Classical ranging method can be classified into the one- way

ranging (OWR) and TWR. The first method can be employed the transceivers which are synchronized to a common clock such as GPS. The second method is enable to the measure of the RTT between two asynchronous transceivers. The technique enabling to measure the signal round-trip Time-Of-Flight (TOF) between two asynchronous transceivers consists in using a classical two-way remote synchronization technique. A pair of terminals are time-multiplexed with half-duplex packet exchanges. This procedure relies on a typical mechanism for fused location and communication: a requestor sends packets to a responder which replies after synchronizing with packets containing synchronous timing information. The reception of this response allows the requestor to determine the round-trip TOF information . Figure 5 shows the two-way raging procedure to measure the distance between two transceivers and its ranging result can be represented by

$$d_{TWR} = T_{OF} \times c \tag{3}$$

where T_{OF} denotes the flight time of RF signal and c is the speed of light. And

$$T_{OF} = 0.5\left(RTT - T_{Reply}\right) \tag{4}$$

Where T_{Reply} indicates the response delay time at the B node.

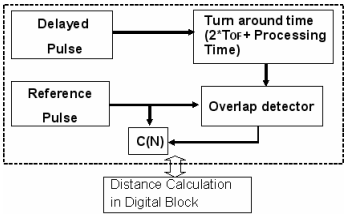

Figure 6. Ranging block diagram.

Generally, in order to measure the TOF, corresponding ranging schemes can be categorized into two major approaches. The first is known as a coherent method, which is carrying out matched filtering using template correlation [18]. The second is non-coherent method, whose major function is designated as the energy detection and collection [9-10]. In this section, to obtain high ranging accuracy in spite of using low clock rate and non-coherent ranging method, sophisticated designed counter-based ranging algorithm is proposed. Figure 6 shows the proposed ranging block diagram which has overlap detector and two clock sources: delayed pulse (f_0) and reference pulse (f_1).

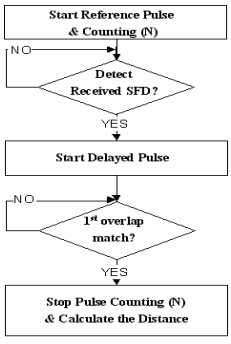

Figure 7. Ranging procedure.

The operation of ranging process is presented in Figure 7. and Figure 8. As shown in Figure 8, at the t_0 moment that TX SFD transmission is begin, the counter starts counting the rising edge of reference pulse until the first overlap occurs. When the RX SFD signal returns via a node at the time t_1, delayed pulse starts. At the time t_2 ,the overlap of two pulses begins and ranging transactions are finished.

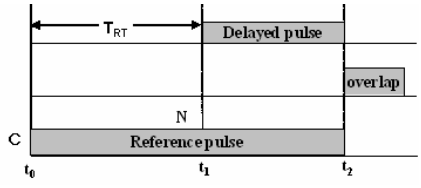

Figure 8. Ranging transactions diagram.

From Figure 8, at the time t_2, can be expressed as the following:

$$t_2 = (N3)/f_1 = T_x + (N1)/f_0 \tag{5}$$

Where N1,N3 is the number of rising edge of delayed pulse and reference pulse, respectively.
And f_0 , f_1 is the frequency of delayed pulse and reference pulse, respectively.
The turn around time is given by

$$T_{RT} = (N3)/f_1 - (N1)/f_0 \tag{6}$$

We define

$$T_{res} = \left|1/f_1 - 1/f_0\right| \tag{7}$$

In case of $T_{res} \le 1\times10^{-9}$ and $T_{RT} << \{1/f_0, 1/f_1\}$, it can be approximated as $N_1 \approx N_3$

Round trip time T_{RT} can be calculated by (8) and the estimated distance is derived as (9). In the equation, τ_0 is the total offset including retranslation delay time.

$$T_{RT} = N \cdot \left|(1/f_1 - 1/f_0)\right| + \tau_0 \tag{8}$$

$$\hat{d} = (T_{RT} - \tau_0) \times C \times 0.5 \tag{9}$$

4. Experimental Ranging Results

Table 1. Experimental Environments.

Parameter	Specification
Channel Bandwidth	2GHz (3-5GHz)
Modulation type	OOK
Receiving type	Envelope Detection
T_b (Bit duration)	1000ns
Spreading code	M-sequence
Code length	15
T_c (Chip duration)	66.7ns
Sampling Freq.	60MHz
Ranging type	TOA /TWR
Positioning type	Triangulation
Area size	18 x 24(m)

In order to verify the complete operation of proposed chaotic communication and ranging scheme, experiments have been conducted in real environments with parameter in Table 1.

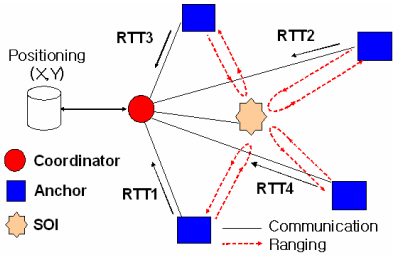

Figure 9. Network Configurations for Ranging & Positioning.

Network Configurations for Ranging & Positioning is shown in Figure 9, In this scheme, four relative distance measurements from a mobile to four references are performed through four distinct full duplex TWR links. A pair of isochronous terminals, viewed as anchors, measure the RTT associated with packets emitted by the SOI (System Of Interest). This configuration leads to the estimation of four RTTs through four distinct TWR transactions. The measured four RTTs are forwarded to server in order to estimate location positioning via coordinator. The position is then calculated with linear regression analysis and classical triangulation methods. For ranging service between two devices based on the conventional IEEE 802.15.4 MAC layer, some management primitives are additionally required.
And to minimize the error caused by delay, SOI should be able to recognize ranging command and the process of command reception should be performed by hardware-MAC.

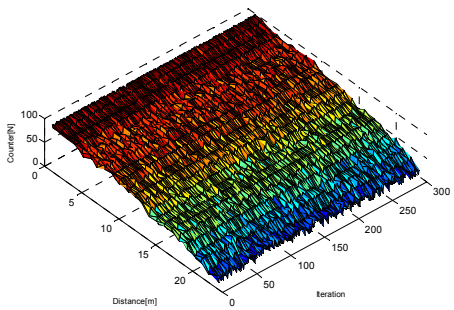

Figure 10. Ranging counter as a function of distance.

Figure 10 shows Ranging counter as a function of distance. It is performed 300 times repetition measurements per 1m distance. As distance increases from 1m to 24m, it is seen that the counter value is proportional lineally with monotonous decreasing.

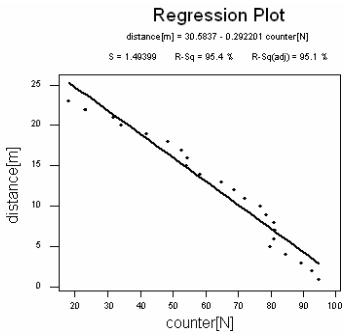

Figure 11. Regression coefficients by linear regression analysis.

Before position estimation, it needs to translate ranging counter value into distance. To do this translation, regression coefficients are calculated by linear regression analysis in Figure 11. Therefore, the distance as a function of ranging counter N is given by

$$\text{distance}[m]=30.5837-0.2922*\text{counter}[N] \qquad (10)$$

A straightforward approach to calculate the position of a mobile terminal based upon TOA uses a geometric interpretation to calculate the intersection of circles for TOA-based algorithms. Indeed, if three TOA are measured between a mobile terminal and three (or more) distinct anchors (note that anchors should be considered as nodes doted with a prior knowledge of their relative positions), the mobile position can be easily computed in the 2-D plane. The position location algorithm estimates the coordinates of node ($\hat{x},\hat{y}$) and obtain the algorithm's performance by computing the distance error between the true and the estimated coordinates is given by.

$$\varepsilon=\sqrt{(x-\hat{x})^2+(y-\hat{y})^2} \qquad (11)$$

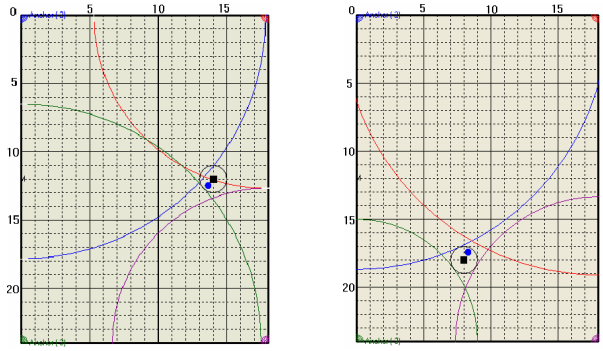

Figure 12. Some examples of true and estimated coordinates . '■' and '●' denotes true and estimate coordinates, respectively.
(a) ■:(14.00,12.00), ●: (13.64,12.47)
(b) ■: (8.00,18.00), ●: (8.32,17.41)

Figure 12 shows some examples of true and estimated coordinates by triangulation position location algorithm in 18(m) x 24(m) indoor area. Where '■' and '●' denotes true and estimate coordinates, respectively.

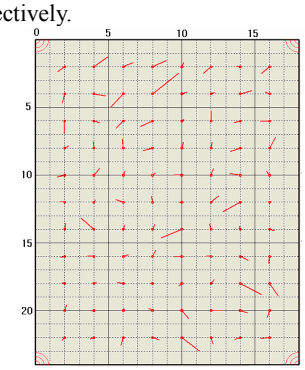

Figure 13. Estimated coordinates connected to true coordinates '•' for the 88 unknown-location SOI.

And, by using of (11), the estimation distance error of Figure 12(a) and 12(b) between the true and the estimated coordinates is

0.5920(m) and 0.6712(m), respectively.

Table 2. Occurrence frequency and percentage by error range.

Error[m]	$\varepsilon \leq 1.0$	$1.0 < \varepsilon \leq 1.5$	$1.5 < \varepsilon \leq 2.0$	$2.0 < \varepsilon \leq 2.5$
Occurrence	78/88	6/88	3/88	1/88
Percentage [%]	88.63	6.81	3.40	1.13

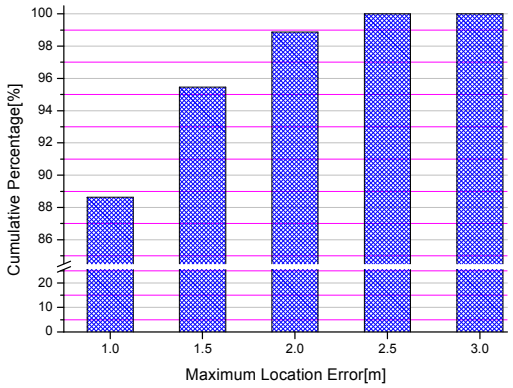

Figure14. Cumulative percentage as a function of maximum location error.

Regarding Figure 13 Table 2 and Figure 14 shows the occurrence frequency and percentage by error range and the cumulative percentage as a function of maximum location error, respectively. In Table 2 and Figure 14, we see that the percentage of less than 1.0m estimation error is more than 88% and the maximum estimation error is less than 1.5m in coverage area more than 95%. And average estimation distance error is about 60cm through total 88 points.

5. Conclusion

In this paper, the feasibility of the ranging application using non-coherent chaotic transceiver has been investigated by designing and implementing the system. To improve ranging accuracy in spite of using low clock rate and non-coherent receiving method, sophisticated designed counter-based ranging algorithm was proposed. In order to verify the complete operation of proposed ranging scheme, its performance has been proved by conducting experiments in real indoor environments. The experiments results have been shown that proposed non-coherent UWB direct chaotic ranging system can find the location of certain SOI unit with network working which operated asynchronously. It is noted the proposed ranging system can be one of the cost effective solutions in the given application field.

Reference

1. Y. Qi, H. Kobayashi and H. Suda, "Unified analysis of wireless geolocation in a non-line-of-sight environment - Part I: analysis of time-of-arrival positioning methods," submitted to IEEE Trans. Wireless Comm., Jan. 2004.
2. Y. Qi, "Wireless geolocation in a non-line-of-sight environment," Ph.D. Thesis, Princeton Univ., Nov. 2003.
3. Neiyer Correal, *Signal Strength Based Ranging*, Motorola, doc 15-04-0564-00-004a
4. Marilynn P. Green, *Sample MAC Requirements for Angle of Arrival Based Ranging*, Nokia, doc 15-04-0563-00-004a
5. Xinrong Li, *Super.Resolution TOA Estimation with Diversity Techniques for Indoor Geolocation Applications*, Ph.D. thesis, Worcester Polytechnic Institute, 2003.
6. E. A. Homier and Robert A. Scholtz, "Rapid acquisition of ultrawideband signals in the dense multipath channel," in *Proc. IEEE 2nd Ultra Wideband Systems and Technologies (UWBST'02)*, May 2002, pp. 245–249.
7. R. Fleming, C. Kushner, G. Roberts, and U. Nandiwada, "Rapid acquisition for ultra-wideband localizers," in *Proc. IEEE 2nd Ultra Wideband Systems and Technologies (UWBST'02)*, May 2002, pp. 105– 109.
8. I. Maravic, M. Vetterli, and K. Ramchandran, "Channel estimation and synchronization with sub-nyquist sampling and application to ultrawideband systems," in *In Proc. ISCAS*, Vancouver, Canada, May, pp. 381–384.
9. M. Weisenhorn and W. Hirt, "Robust noncoherent receiver exploiting UWB channel properties," in *Proc. Joint UWBST&IWUWBS*, May 2004, vol. 2, pp. 156–160.
10. A. Rabbachin, R. Tesi, and I. Oppermann, "Bit error rate analysis for UWB systems with a low complexity, non-coherent energy collection receiver," in *Proc. IST Mobile & Wireless Communications Summit*, Lyon, France, June 2004, vol. 2.
11. M.S. Win and R.A. Scholtz, "Impulse Radio: How it works", *IEEE Comm.,.Letter.*, Vol. 2, No. 1, 1998, pp. 10-12.
12. Robert J. Fontana, Steven J. Gunderson, "Ultra-Wideband Precision Asset Location System", Proceedings IEEE Conference on Ultra Wideband Systems 2002.
13. IEEE 802.15.4a, "Merged UWB proposal for IEEE 802.15.4a Alt-PHY," *http://www.ieee802.org/15/pub/TG4a.html* IEEE 15-05-0158-00-004a, March 2005
14. IEEE 802.15.4a, "Merged Proposal of Chaotic UWB System for 802.15.4a," *http://www.ieee802.org/15/pub/TG4a.html* IEEE 15-05-0132-03-004a, March 2005
15. A.S. Dmitriev, B. Kyarginsky, A. Panas, and S. Starkov, "Direct Chaotic Communication System Experiments", *Proc. 9th Workshop on Nonlinear Dynamics of Electronic Systems (NDES'2001), Delft, Netherlands*, June 21-23, 2001, pp. 185-188
16. Rulkov, N.F.; Sushchik, M.M.; Tsimring, L.S.; Volkovskii, A.R.," Digital communication using chaotic-pulse-position modulation", Circuits and Systems I: Fundamental Theory and Applications Vol. 48, Issue 12, Dec. 2001 , 9 pp.
17. Chia-Chin Chong; Su Khiong Yong; Seong Soo Lee; "UWB direct chaotic communication technology", Antennas and Wireless Propagation Letters ,Vol. 4, 2005 pp.316 – 319
18. I. Nygren and M. Jansson, "Robust Terrain Navigation with the Frame Correlation Method for High Position Accuracy," Proc. IEEE Conference on OCEANS 2003, vol. 3, May 2003.